Journal of Solid State Chemistry **167,** 196–202 (2002)
doi:10.1006/jssc.2002.9642

A Novel Complex Cobalt Gallium Oxide $Ca_2Co_{0.8}Ga_{1.2}O_{4.8}$: Synthesis and High-Temperature Electron Transport Properties

S. Ya. Istomin,*[,1] E. V. Antipov,* G. Svensson,† J. P. Attfield,† V. L. Kozhevnikov,§ I. A. Leonidov,§ M. V. Patrakeev,§ and E. B. Mitberg§

*Department of Chemistry, Moscow State University, 119899 Moscow, Russia; †Department of Structural Chemistry, Stockholm University, SE-10691 Stockholm, Sweden; ‡Deptartment of Chemistry, University of Cambridge, Lensfield Road, Cambridge CB2 1EW, United Kingdom; and §Institute of Solid State Chemistry, Ural Branch of RAS, 620219 Ekaterinburg, Russia

Received January 31, 2002; in revised form April 26, 2002; accepted May 3, 2002

A new complex oxide with the cation ratio Ca:Co:Ga = 2:0.8:1.2 has been synthesized in air at 1150°C. The cobalt atoms adopt oxidation states 2+ and 3+ in equal amounts giving an oxygen content corresponding to the composition $Ca_2Co_{0.8}Ga_{1.2}O_{4.8}$. It crystallizes in *F*-centered cubic structure with $a = 15.0558$ Å. Conductivity measurements performed at high temperatures revealed that the temperature increase gives a charge disproportionation of Co^{3+} species resulting in a small concentration of Co^{4+} species and thus a small p-type conductivity in the oxide. A decrease of the oxygen pressure promotes oxygen depletion from the oxide and a deterioration of the conductivity. The electric properties are interpreted within a small polaron conduction mechanism. An unusually large mobility activation energy of 0.45 eV can be explained by a large spatial separation of cobalt cations in the structure.

Key Words: **complex oxides; electron-diffraction; electron-transport properties; X-ray powder diffraction.**

INTRODUCTION

Complex iron and cobalt oxides attract researchers' attention as materials having a variety of interesting properties. Many of these oxides are mixed conductors, i.e., they are able to simultaneously conduct oxygen ions and electrons at elevated temperatures and, thus, can be used in design of electrodes for solid oxide fuel cells (SOFCs), membranes for separation of oxygen from gaseous mixtures, etc. A considerable amount of data exists concerning structural peculiarities, thermodynamics and conducting properties of perovskite-like phases in the system La–*A*–Co–Fe–O, where *A* is an alkali-earth metal (1). Other structural types are studied less extensively. There are indications in the literature that oxygen vacancy ordered phases in the La–*A*–Fe–Ga–O system may have significant mixed conductivity at high temperatures (2–4). At the same time, there are no data regarding vacancy-ordered cobaltites.

The brownmillerite structure is one of the examples of oxygen vacancy ordering in the oxygen-deficient compounds with a perovskite structure. Complex oxides $A_2BB_2'O_5$ with a brownmillerite structure are known to exhibit high oxide-ion conductivity. For example, $Ba_2In_2O_5$ has a conductivity of $\sim 10^{-3}$ S/cm (800°C) that jumps to 10^{-1} S/cm above an order–disorder transition (5).

We have searched for new complex cobalt oxides with a brownmillerite structure in the Ca–Ga–Co–O system. In this work, we present synthesis and high-temperature electron transport properties of a new oxide $Ca_2Co_{0.8}Ga_{1.2}O_{4.8}$.

EXPERIMENTAL

Pelletized mixtures of high-purity grade $CaCO_3$, Co_3O_4 and Ga_2O_3 were used in the synthesis. The pellets were fired in air and nitrogen at 1100–1150°C for 20–48 h. Iodometric titration was used to determine the oxygen content in as-prepared samples. About 50 mg of the sample under investigation was placed in a flask containing 20 ml of a 20% water solution of KI. Then, several drops of concentrated HCl were added to the solution. The flask was kept in a dark place until dissolution of the entire sample. The released elementary iodine was titrated by a standard $Na_2S_2O_3$ solution with starch added as an indicator. The ability of the as-synthesized specimens to reversibly lose oxygen was studied in a Setaram

[1] To whom correspondence should be addressed. Fax: +7-095-939-47-88. E-mail: istomin@icr.chem.msu.ru.

0022-4596/02 $35.00

TG-DTA-92 thermoanalyzer by heating the sample in a flow of helium ($pO_2 = 10^{-3}$ atm).

X-ray powder diffraction (XRD) patterns of specimens were recorded with an FR-552 focusing camera using Cu$K\alpha_1$ radiation and germanium as an internal standard ($a = 5.6574$ Å). X-ray powder diffractometer data were collected in symmetric transmission mode on a STOE STADI-P powder diffractometer equipped with a mini-PSD detector.

Electron diffraction studies (ED) were carried out with a JEOL JEM 2000 FX instrument operated at 200 kV. Small amounts of the samples were crushed in *n*-butanol and used in the transmission electron microscopy (TEM) studies. A drop of this dispersion was put on a holey carbon film supported by a copper grid. Microanalyses of the individual crystallites for the determination of cation content on the same grids as studied in the TEM were performed with a JEOL JSM 880 scanning electron microscope equipped with a windowless energy-dispersive analyser (EDS) LINK *Isis*.

Rectangular bars $2 \times 2 \times 18$ mm were cut from the sintered pellets for electrical measurements. One specimen, equipped with butt electrodes and thermocouples, was used for measurements of the thermopower α. The temperature gradient along the sample was about 15 K/cm. Another specimen was used in four-probe measurements of the d.c. conductivity σ. The current leads were tightly wound to the sample at 16 mm spacing while the spacing between potential probes was 10 mm. The specimen was placed perpendicular to the specimen for thermopower measurements so that the temperature gradient along the sample was zero. The measurements of conductivity and thermopower were carried out simultaneously in a cell utilizing oxygen sensing and pumping properties of cubically stabilized zirconia oxygen electrolyte as described elsewhere (6). The cell was filled with a 50% O_2, 50% CO_2 gas mixture in the beginning of the experiment and sealed. A typical value of the pump current necessary to maintain a desirable oxygen pressure inside the cell did not exceed 0.5 mA. The electrical parameters were measured with a high-precision Solartron 7081 voltmeter. The experimental data points were collected after equilibrium had been reached between the sample and ambient oxygen gas. Equilibrium state was assumed to have been attained when changes in the logarithm of the conductivity did not exceed 0.1%/min and changes in thermopower did not exceed 0.001 μV/min. The measurements were carried out as isothermal runs. Thermopower data were corrected for the contribution of the platinum leads (7).

Magnetization measurements were recorded with a SQUID magnetometer (MPMS 2 Quantum Design) as a function of temperature under a magnetic field of 1000 G on field-cooled powdered samples. Susceptibility values were corrected for the diamagnetic contribution.

RESULTS AND DISCUSSION

Synthesis

A new phase having nominal composition Ca_2CoGaO_x was detected in the sample that had been annealed at 1100°C for 24 h either in nitrogen or in air. XRD showed also the presence of approximately 15% of CaO and 15% of CoO in the sample. The EDX analysis suggested the cation composition of the new phase to be Ca:Ga:Co = 51(2):30(2):19(1) at%. in considerable difference to the nominal composition Ca:Ga:Co = 50:25:25 at%. In order to obtain a single-phase specimen, compositions $Ca_2Ga_{1.2}Co_{0.8}O_x$, $Ca_2Ga_{1.1}Co_{0.9}O_x$ and $Ca_{2.2}Ga_{1.2}Co_{0.8}O_x$ were annealed at 1100°C for 24 h in air, however, the samples still contained impurity phases as CaO, $Ca_3Ga_4O_9$ and Co_3O_4. Further annealing at 1100°C did not produce single-phase specimens. However, at 1150°C a single-phase sample was obtained for $Ca_2Ga_{1.2}Co_{0.8}O_x$. Thus, the conclusion can be drawn that this nominal composition correctly reflects the cation ratio in the new phase. Firing of the other compositions, $Ca_2Ga_{1.1}Co_{0.9}O_x$ and $Ca_{2.2}Ga_{1.2}Co_{0.8}O_x$, resulted in samples containing about 10 at% of admixture phases. Further studies indicated that the compound has a homogeneity range revealed as a variation of the *a*-axis with composition. The oxygen content in $Ca_2Ga_{1.2}Co_{0.8}O_x$, as determined by the iodometric titration, was found to correspond to $x = 4.8$. Hence, the average oxidation state of cobalt is $+2.5$, and equal amounts of Co^{2+} and Co^{3+} cations reside in the as-prepared phase $Ca_2Ga_{1.2}Co_{0.8}O_{4.8}$.

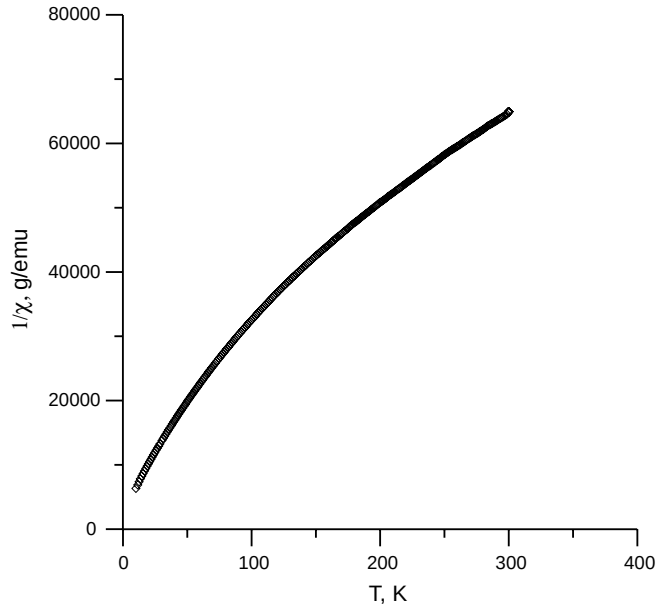

FIG. 1. Temperature dependence of the reciprocal magnetic susceptibility for $Ca_2Ga_{1.2}Co_{0.8}O_{4.8}$.

Measurements of the magnetic susceptibility versus temperature indicated a paramagnetic behavior, however, with a non-linear dependence of $1/\chi(T)$ (Fig. 1). The calculated effective magnetic moment per cobalt atom in $Ca_2Ga_{1.2}Co_{0.8}O_{4.8}$ is 3.65 μ_B at 300 K. This suggests that both the Co^{2+} and Co^{3+} are in high spin states (The ideal spin-only magnetic moments for high spin (HS) or low-spin (LS) moments are: Co^{2+} (LS), Co^{2+} (HS) and Co^{3+} (LS), Co^{3+} (HS), Co^{3+} (intermediate states (IS), $t_{2g}^5 e_g^1$) are 1.73, 3.87 and 0, 4.90, 2.83 μ_B). At 300 K and in oxygen surroundings, cobalt is most probably in HS or IS (Co^{3+}) states. Hence, taking into account that compound contains equal amounts of Co^{2+} and Co^{3+} the calculated relative amounts of different spin states are 0.5 Co^{2+} (HS), 0.14 Co^{3+} (HS) and 0.36 Co^{3+} (IS).

X-Ray and Electron Diffraction Study

The low 2Θ region of the X-ray powder diffraction pattern for $Ca_2Ga_{1.2}Co_{0.8}O_{4.8}$ is shown in Fig. 2. The XRD pattern can be indexed in a *F*-centered cubic unit cell with $a = 15.0558(3)$ Å. The unit-cell dimensions and reflection intensities suggest a perovskite-related structure with $a = 4 \times a_{per}$ ($a_{per} = 3.76$ Å). No systematic absence of reflections was found except for the *F*-centering ones. The *F*-centered unit cell was confirmed by the selected-area electron diffraction (SAED). The SAED patterns taken along ⟨100⟩ and ⟨110⟩ directions of one of the microcrystals are shown in Figs. 3a and 3b, respectively. The cubic symmetry could be confirmed by the observation of the three-fold axis in ⟨111⟩ CBED pattern as shown in Fig. 4. Consequently, the structure of $Ca_2Ga_{1.2}Co_{0.8}O_{4.8}$ may be described within space groups *F*23 (196), *Fm*-3 (202), *F*432 (209), *F*43*m* (216) and *Fm*3*m* (225). A detailed study of the crystal structure of $Ca_2Ga_{1.2}Co_{0.8}O_{4.8}$ using neutron diffraction data is under progress and will be reported elsewhere.

The double perovskites $A_2BB'O_6$ can often accommodate considerable amount of oxygen vacancies. The ordered arrangement of oxygen vacancies favors crystallization of such oxides in the brownmillerite-type structure. Examples are Ca_2MnGaO_5 (8), Sr_2MnGaO_5 (9), Ca_2FeGaO_5 (10), and Ca_2FeAlO_5 (11). The brownmillerite structure is characterized by alteration of layers of corner-sharing octahedra BO_6 and layers of $B'O_4$ tetrahedra where structural vacancies are located. It is

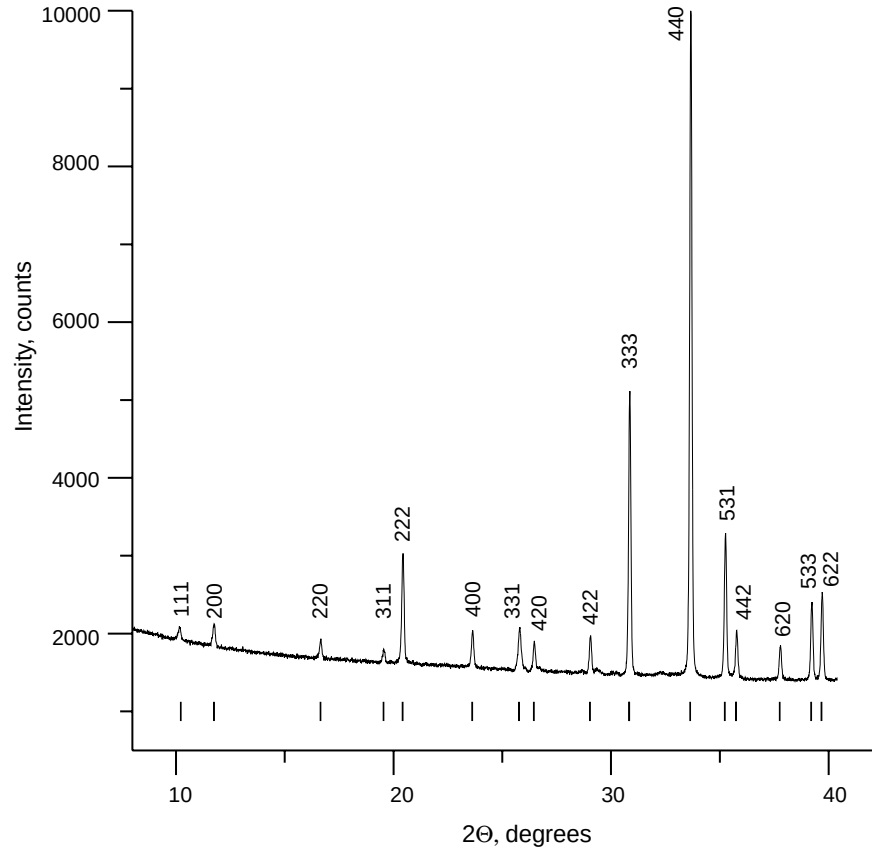

FIG. 2. XRD pattern of $Ca_2Ga_{1.2}Co_{0.8}O_{4.8}$.

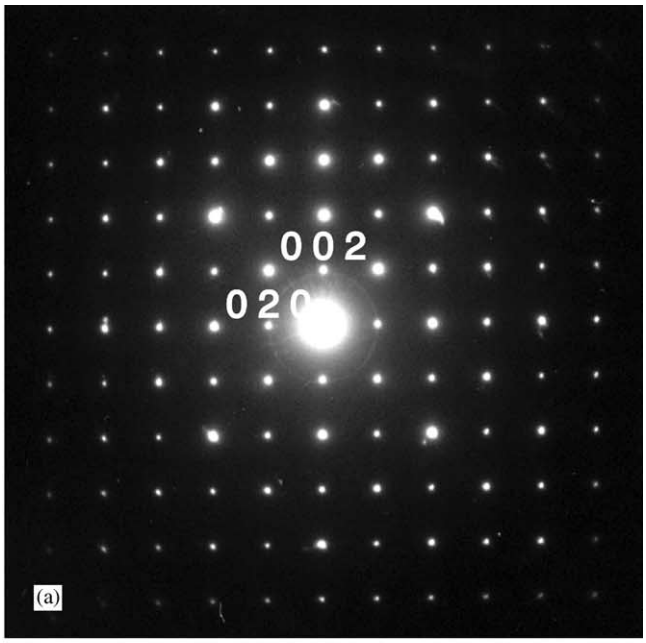

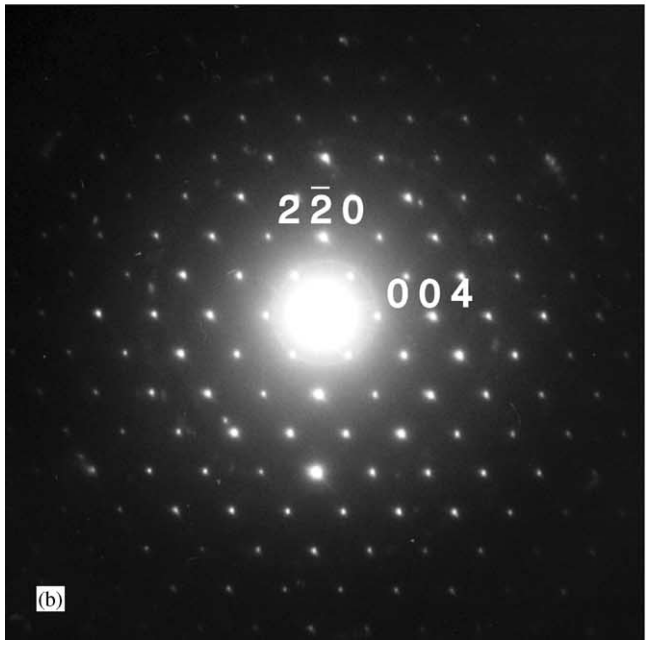

FIG. 3. SAED patterns of a crystallite viewed along (a) ⟨100⟩ and (b) ⟨110⟩. Two reflections in each pattern are indexed with the *F*-centered unit cell $a = 15.0558$ Å.

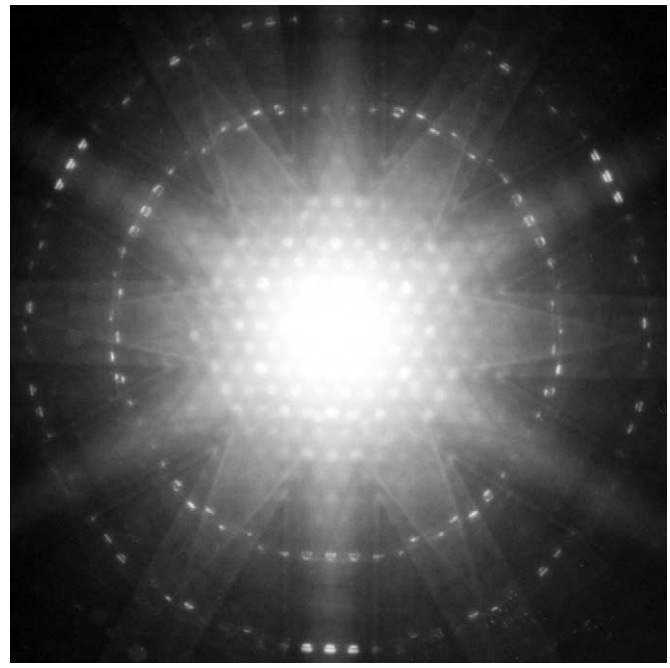

FIG. 4. CBED bright field (BF) and whole pattern (WP) of a crystallite viewed along ⟨111⟩.

interesting to note that though Mn and Fe do form brownmillerite-type oxides Ca_2MnGaO_5 and Ca_2FeGaO_5, their neighbor in periodic table Co promotes crystallization of another structure with a very close calcium and gallium content. It is seen from the obtained results that the brownmillerite-like oxide Ca_2CoGaO_5 comprising only Co^{3+} cations does not exist. Instead, a different ratio of the *B*-cations and oxygen is adopted to form isotropic perovskite-like structure of $Ca_2Co_{0.8}Ga_{1.2}O_{4.8}$, where Co^{2+} and Co^{3+} cations are in equal amounts. The peculiar feature of the structure is large elementary unit with $a \approx 15$ Å. To our knowledge, structural analogs for $Ca_2Co_{0.8}Ga_{1.2}O_{4.8}$ are unknown. The reason for such structural difference may be in the stability of the 3+ oxidation state, which is known to decrease from Mn to Fe and Co, thus disfavoring formation of the Ca_2GaCoO_5 brownmillerite.

Transport Properties

The plots at different temperatures of electrical conductivity (σ) and thermopower (α) versus oxygen partial pressure are shown in Figs. 5 and 6, respectively. The positive sign of thermopower is indicative of electron holes (h^+) being the majority carriers. The conductivity increases and the thermopower decreases, both demonstrate that the hole concentration increases with oxygen pressure pO_2. Small values of conductivity and rather large values of thermopower both reflect low concentration and mobility of hole carriers.

The hole conductivity is usually related to the presence of Co^{4+} ions in cobaltites (12). However, the charge neutrality requirement is consistent with the formula $Ca_2^{2+}Co_{0.8-2\delta}^{3+}Co_{2\delta}^{2+}Ga_{1.2}^{3+}O_{5-\delta}^{2-}$ of the compound where there are no Co^{4+} species. A supposition seems plausible that some amount of Co^{4+} ions appears in the oxide as a result

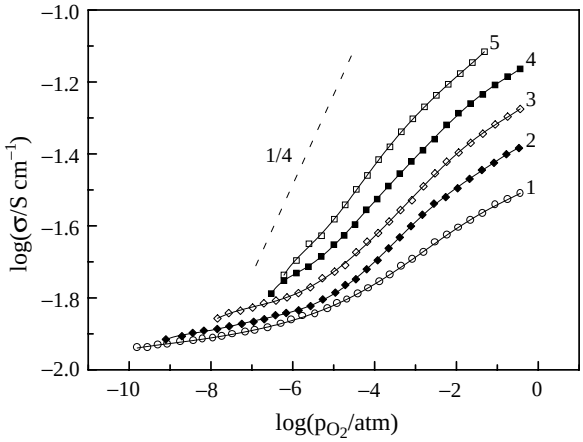

FIG. 5. Dependence of the conductivity in $Ca_2Ga_{1.2}Co_{0.8}O_{4.8}$ on partial pressure of oxygen at different temperatures (1) 750°C, (2) 800°C, (3) 850°C, (4) 900°C, and (5) 950°C.

of the charge disproportionation reaction

$$2Co^{3+} \leftrightarrow Co^{4+} + Co^{2+}, \qquad [1]$$

which is common in cobalt-containing perovskite-like oxides. The equilibrium constant for this reaction is

$$K_1 = \frac{[Co^{4+}][Co^{2+}]}{[Co^{3+}]^2} = K_1^0 \exp\left(-\frac{\Delta H_1}{k_B T}\right) \qquad [2]$$

It may seem from Eq. [2] that the concentration $[Co^{4+}]$ depends on temperature only. However, this is an oversimplification as the oxygen exchange reaction

$$O^{2-} + 2Co^{3+} \leftrightarrow 2Co^{2+} + \tfrac{1}{2}O_2 \qquad [3]$$

indirectly influences concentration of Co^{4+} species. Using the corresponding equilibrium constant

$$K_2 = \frac{[Co^{2+}]^2 pO_2^{1/2}}{[Co^{3+}]^2[O^{2-}]} = K_2^0 \exp\left(-\frac{\Delta H_2}{k_B T}\right) \qquad [4]$$

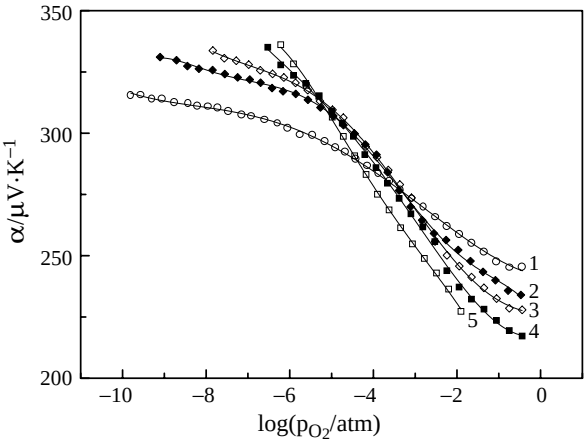

FIG. 6. Dependence of the thermopower in $Ca_2Ga_{1.2}Co_{0.8}O_{4.8}$ on partial pressure of oxygen at different temperatures: (1) 750°C, (2) 800°C, (3) 850°C, (4) 900°C, and (5) 950°C.

in combination with K_1 in Eq. [2], one can find the dependence of the Co^{4+} concentration upon oxygen pressure and temperature as

$$[Co^{4+}] = K_1^{\circ}(K_2^{\circ})^{-1/2}\frac{[Co^{3+}]}{[O^{2-}]^{1/2}} pO_2^{1/4} \exp\left(-\frac{\Delta H_1 - \Delta H_2/2}{k_B T}\right). \qquad [5]$$

It follows from Eq. [5] that $[Co^{4+}]$ must vary with oxygen pressure proportionally to $pO_2^{1/4}$ when the pressure dependence of either $[Co^{3+}]$ or $[O^{2-}]$ can be neglected. In fact, the slopes of the isotherms $\sigma - pO_2$ in Fig. 5 are smaller than $\frac{1}{4}$ and, moreover, they depend on pO_2. Therefore, we have to infer that the pressure dependence of $[Co^{3+}]$ and $[O^{2-}]$ cannot be disregarded. This conclusion is quite consistent with a substantial involvement of the oxygen exchange reaction (as evidenced by TG) in the overall equilibrium balance of charged species. In general, the pressure and temperature dependencies of electric properties in the oxygen deficient oxide $Ca_2Co_{0.8}Ga_{1.2}O_{5-\delta}$ demonstrate behavior typical of a semiconductor in the regime of extrinsic conductivity.

The relation between thermopower α and $\lg\sigma$ in the extrinsic regime of conductivity can be found from the known equations

$$\sigma = q\mu p \qquad [6]$$

and

$$\alpha = \frac{k_B}{q} \ln \frac{N}{p}. \qquad [7]$$

Here, q is the absolute value of the elementary charge (e^-), μ and p represent mobility and volume concentration of holes, respectively, N is the volume concentration of sites available for holes and k_B is the Boltzman constant.

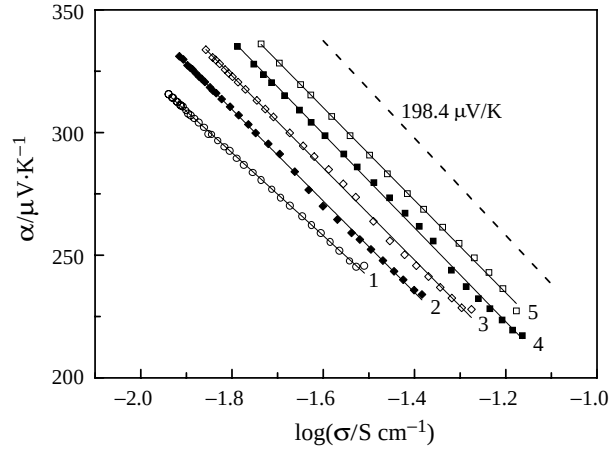

FIG. 7. Dependence of the thermopower of $Ca_2Ga_{1.2}Co_{0.8}O_{4.8}$ versus conductivity (in logarithmic scale) at different temperatures: (1) 750°C, (2) 800°C, (3) 850°C, (4) 900°C, and (5) 950°C.

Combining Eqs. [6] and [7] results in

$$\alpha = \frac{k_B}{q \ln 10}(\lg(N\mu q) - \lg(\sigma)), \quad [8]$$

where $k_B/(q\ln 10) = 198.4\,\mu V/K$. Here found of the isotherms $\alpha - \lg\sigma$ correspond to this value perfectly well as seen in Fig. 7. Assuming temperature-activated hole mobility, we can rewrite Eq. [6] in the form

$$\sigma = qp\frac{\mu^0}{T}\exp\left(-\frac{U}{k_B T}\right), \quad [9]$$

where μ^0 is the mobility pre-exponent and U is the mobility activation energy. Note that constant values of thermopower roughly correspond to constant values of the hole concentration. More precisely, α = constant when N/p = constant where N may generally depend on p. However, we neglect this dependence, which can become substantial at large concentration of holes, and accept that changes in α are mainly related to changes in concentration of holes. Thus, the isoelectric plots of conductivity, i.e., plots of conductivity at fixed values of thermopower versus $1/T$, enable evaluation of the mobility activation energy. Such Arrhenius plots are shown in Fig. 8. A mobility activation energy equal to 0.45 eV can be obtained from these plots. The experimental values of the pre-exponential multiplier $\sigma^0 = qp\mu^0$ decrease linearly with increasing thermopower, i.e., with the removal of holes. This behavior is consistent with Eqs. [6] and [7]. Indeed, the thermopower is proportional to $-\lg p$ and, thus, it changes as $-p$ at small values of the hole concentration while σ is proportional to p by definition. The temperature–activated mobility of holes in $Ca_2Co_{0.8}Ga_{1.2}O_{5-\delta}$ is a direct evidence for electron transport via hopping of small polarons. However, the migration activation energy is unusually large in $Ca_2Co_{0.8}Ga_{1.2}O_{5-\delta}$ compared to perovskite-type oxides containing cobalt only in the *B*-sublattice. For instance, the mobility activation energy equals only to about 0.08 eV in $La_{0.4}Sr_{0.6}CoO_{3-\delta}$ (13). Such a large energy necessary for the transfer may reflect the influence of a peculiar structural architecture in $Ca_2Co_{0.8}Ga_{1.2}O_{5-\delta}$ on the polaron migration pathway. Indeed, the polaron movement in perovskite-like cobaltites, e.g., $La_{1-x}Sr_xCoO_{3-\delta}$, occurs via jumps of a polaron from a Co^{4+} ion to a Co^{3+} ion, which are facilitated by an oxygen ion in between neighboring Co^{4+} and Co^{3+} ions, i.e., according to the scheme $\cdots \to Co^{4+} \to O^{2-} \to Co^{3+} \to \cdots$ The situation is different in $Ca_2Co_{0.8}Ga_{1.2}O_{5-\delta}$ where less than a half of *B*-sites is occupied by cobalt ions and the shortest paths in the structure from one Co^{4+} ion to an adjacent Co^{3+} ion seem to more often involve two oxygen ions, i.e., it can be depicted as $\cdots \to Co^{4+} \to O^{2-} \to O^{2-} \to Co^{3+} \to \cdots$ This migration pathway is both longer and energetically less favorable and, thus, leads to a larger apparent activation energy for the migration.

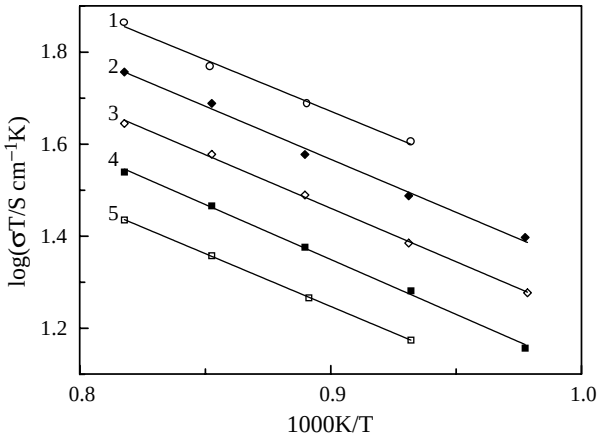

FIG. 8. Isoelectric plots of conductivity with Arrhenius coordinates: (1) 240, (2) 260, (3) 280, (4) 300, and (5) 320 μV/K.

Taking in view the residence of Co^{2+}, Co^{3+} and Co^{4+} in the oxide, its' formula can be written as $Ca_2^{2+}Co_x^{2+}Co_y^{3+}Co_z^{4+}Ga_{1.2}^{3+}O_{5-\delta}^{2-}$. The site balance can be expressed as

$$x + y + z = 0.8. \quad [10]$$

The electroneutrality requirement is

$$2 \times 2 + 2x + 3y + 4z + 1.2 \times 3 = 2(5 - \delta), \quad [11]$$

which in combination with Eq. [10] gives

$$y + 2z = 0.8 - 2\delta. \quad [12]$$

The general relation [7] for thermopower may be written in these notations as

$$\alpha = \frac{k_B}{q}\ln\frac{y}{z}. \quad [13]$$

Hence, concentration of holes can be expressed from Eqs. [12] and [13] as

$$z = \frac{(0.8 - 2\delta)}{2 + 10^{\alpha/198.4}}. \quad [14]$$

The experimental value of δ, as obtained from TG measurements, is equal to 0.27 at 850°C and $pO_2 = 10^{-3}$ atm. Hence, the concentration of holes in these conditions can be calculated from Eq. [14] as $z = 0.01$ while α values are taken from the experimental data presented in Fig. 6. Then, from Eq. [6] we can evaluate the mobility of holes at 850°C as $\mu_{850^\circ C} = 0.0021\,cm^2/V \cdot s$. When the concentration of charge carriers is small, their mobility can be approximated by the known expression $\mu = (\mu^0/T)\exp(-U/k_B T)$. Therefore, using $\mu_{850^\circ C}$ and the activation energy $U = 0.45\,eV$, we can estimate $\mu^0 \approx 225\,cm^2 \cdot K/V\,s$. Then, the variations of x, y and z with pO_2 at different temperatures can be calculated from Eqs. [6], [10], [12] and [13]. The calculated concentrations of cobalt species are shown in Fig. 9. The changes in

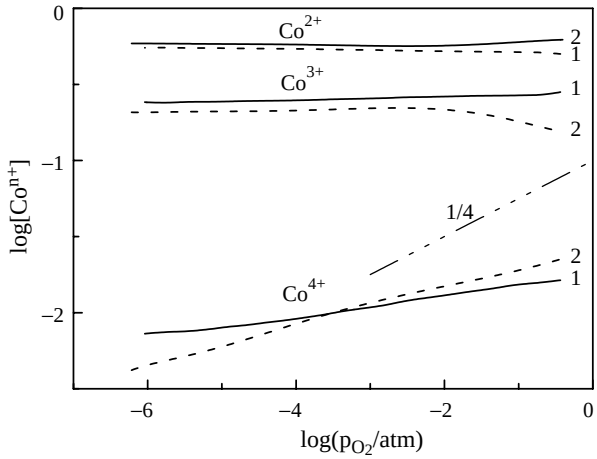

FIG. 9. Dependence of the concentrations of different oxidation states of cobalt on partial pressure of oxygen at different temperatures: (1) 750°C and (2) 950°C.

oxygen content calculated with Eq. [12] are shown in Fig. 10. It is clearly seen in Fig. 9 that in the high-pressure limit, the concentration of Co^{3+} ions decreases with the temperature increase while concentrations of Co^{2+} and Co^{4+} ions increase. These changes are quite in accord with the equilibrium constant [2] for reaction [1]. However, in the oxygen pressure range below about 10^{-4} atm, the concentration of Co^{4+} is smaller at 950°C than at 750°C. This deviation can be understood as a consequence of the oxygen depletion reaction

$$Co^{4+} + O^{2-} \rightarrow Co^{2+} + 0.5O_2. \qquad [15]$$

The intensity of this reaction decreases both with temperature and increasing oxygen pressure thus leading to a less strong dependence of oxygen content and, consequently, concentration of holes in $Ca_2Co_{0.8}Ga_{1.2}O_{5-\delta}$ at low oxygen pressures. As a result, the amount of Co^{4+} ions is somewhat larger in the oxide at 750°C compared to 950°C in the low-pressure range.

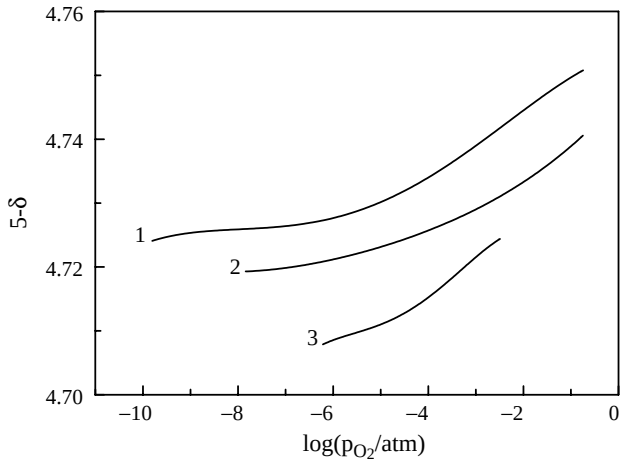

FIG. 10. Dependence of the oxygen content in $Ca_2Co_{0.8}Ga_{1.2}O_{5-\delta}$ on partial pressure of oxygen at different temperatures: (1) 750°C, (2) 850°C, and (3) 950°C.

The obtained data on concentration and mobility of hole carriers in $Ca_2Co_{0.8}Ga_{1.2}O_{5-\delta}$ are in reasonable correspondence with respective data for other typical small polaron conductors. When comparing the results with the data for the perovskite-like cobaltite $La_{0.4}Sr_{0.6}CoO_{3-\delta}$, we see that both hole mobility and concentration of holes are about two orders of magnitude smaller in $Ca_2Co_{0.8}Ga_{1.2}O_{5-\delta}$. This difference results in more than four orders of magnitude smaller conductivity in $Ca_2Co_{0.8}Ga_{1.2}O_{5-\delta}$ compared to $La_{0.4}Sr_{0.6}CoO_{3-\delta}$.

ACKNOWLEDGMENTS

This research was partly supported by Royal Society (UK) through a Joint Research Project and The Royal Swedish Academy of Sciences (KVA). The authors are also thankful to the Russian Foundation for Basic Research (Grants 01-03-96519, 02-02-06450 and 02-03-32990), the Swedish Research Council and INTAS program (Grant 01-00278).

REFERENCES

1. H. J. M. Bouwmeester and A. J. Burggraaf, *in* "Fundamentals of Inorganic Membrane Science and Technology" (A. J. Burggraaf and L. Cot, Eds.), p. 435 and references therein. Elsevier, Amsterdam, 1996.
2. M. Shwartz, J. White, and A. Summels, Int. Patent Application PCT WO 97/41060. 1997.
3. V. L. Kozhevnikov, I. A. Leonidov, M. V. Patrakeev, E. B. Mitberg, and K. R. Poeppelmeier, *J. Solid State Chem.* **158,** 320 (2000).
4. I. A. Leonidov, V. L. Kozhevnikov, E. B. Mitberg, M. V. Patrakeev, V. V. Kharton, and F. M. B. Marques, *J. Mater. Chem.* **11,** 1201 (2001).
5. J. B. Goodenough, J. E. Ruiz-Diaz, and Y. S. Zhen, *Solid State Ionics* **44,** 21 (1990)
6. E. B. Mitberg, M. V. Patrakeev, A. A. Lakhtin, I. A. Leonidov, V. L. Kozhevnikov, and K. R. Poeppelmeier, *J. Alloys Compd.* **274,** 103 (1998).
7. N. Cusak and P. Kendall, *Proc. Phys. Soc.* **72**, 898 (1958); V. D. Barbanyagre, T. I. Timoshenko, A. M. Illyinets, and V. M. Shamshurov, Powder Diffraction **12,** 22 (1997).
8. A. M. Abakumov, M. G. Rozova, B. Ph. Pavlyuk, M. V. Lobanov, E. V. Antipov, O. I. Lebedev, G. Van Tendeloo, D. V. Sheptyakov, and A. M. Balagurov, *J. Solid State Chem.* **158,** 100 (2001).
9. A. M. Abakumov, M. G. Rozova, B. Ph. Pavlyuk, M. V. Lobanov, E. V. Antipov, O. I. Lebedev, G. Van Tendeloo, O. I. Ignatchik, E. A. Ovtchenkov, Yu. A. Koksharov, and A. N. Vasilév, *J. Solid State Chem.* **160,** 353 (2001).
10. R. Arpe, R. von Schenck, and Hk. Mueller-Buschbaum, *Z. Anorg. Allg. Chem.* **410,** 97 (1974).
11. A. A. Colville and S. Geller, *Acta Crystallogr. B* **27,** 2311 (1971)
12. S. R. Sehlin, H. U. Anderson, and D. M. Sparlin, *Phys. Rev. B* **52,** 11681 (1995).
13. E. B. Mitberg, M. V. Patrakeev, I. A. Leonidov, V. L. Kozhevnikov, and K. R. Poeppelmeier, *Solid State Ionics* **130,** 325 (2000).